GEOLOGY | THE GEOLOGICAL SOCIETY OF AMERICA®

https://doi.org/10.1130/G46710.1

Manuscript received 1 July 2019
Revised manuscript received 10 October 2019
Manuscript accepted 15 October 2019

Published online 22 November 2019



# Lithosphere thickness controls continental basalt compositions: An illustration using Cenozoic basalts from eastern China

Pengyuan Guo[1,2]*, Yaoling Niu[1,2,3,4], Pu Sun[1,2], Hongmei Gong[1,2] and Xiaohong Wang[1,2]
[1]Key Laboratory of Marine Geology and Environment, Institute of Oceanology, Chinese Academy of Sciences, Qingdao 266071, China
[2]Qingdao National Laboratory for Marine Science and Technology, Qingdao 266061, China
[3]Department of Earth Sciences, Durham University, Durham DH1 3LE, UK
[4]School of Earth Science and Resources, China University of Geosciences, Beijing 100083, China

## ABSTRACT

**Recent studies demonstrate that lithosphere thickness variation exerts the primary control on global seafloor basalt compositions. If the mechanism of such control, i.e., the lid effect, is indeed at work, lithosphere thickness variation must also influence basaltic compositions in continental settings. To test this hypothesis, we chose to study Cenozoic basalts in eastern continental China over a distance of ~260 km along a southeast-to-northwest traverse with a steep topographic gradient (~500 to ~1500 m above sea level) mirrored with a steep lithospheric thickness gradient (~80 to ~120 km). The basalts erupted on the thinned lithosphere to the east are characterized by lower pressure (e.g., higher $Si_{72}$, lower $Mg_{72}$, $Fe_{72}$, and $[Sm/Yb]_N$; subscript "72" refers to corresponding oxides corrected for fractionation effect to Mg# = 72; N—primitive mantle normalized) and higher extent (e.g., low $Ti_{72}$, $P_{72}$, $K_{72}$, Rb, Ba, Th, and ratios of more- to less-incompatible elements such as $[La/Sm]_N$, Ba/Zr, and Zr/Yb) of melting than basalts erupted on the thickened lithosphere to the west. Importantly, these geochemical parameters all show significant correlations with both lithosphere thickness and topographic elevation. These first-order observations are a straightforward manifestation of the lid effect. Lithospheric contamination and mantle-source compositional variation can indeed contribute to the compositional variability of these continental basalts, but these latter effects are averaged out and are overshadowed by the lid effect. This finding emphasizes the importance of evaluating the lid effect before interpreting the petrogenesis of continental basalts and mantle dynamics. Our results also indicate that the continental surface elevation is isostatically balanced above a mantle depth that is deeper than the lithosphere-asthenosphere boundary.**

## INTRODUCTION

Basaltic magmas produced in continental settings have large compositional variations: petrologically from tholeiites to varying alkali-rich basalts (e.g., Dupuy and Dostal, 1984; Bell and Peterson, 1991; Guo et al., 2016). While factors such as source compositional variation (e.g., Lum et al., 1989), fractional crystallization (e.g., Peterson, 1989), and crustal contamination (Dupuy and Dostal, 1984; Ingle et al., 2004) can all affect erupted basalt compositions, the lithosphere thickness effect on the compositional variation of continental basalts has been largely overlooked, despite some speculation about lithospheric affects on the abundance and patterns of rare earth elements in oceanic basalts by Ellam (1992) and other studies, and implications in experimental petrology (e.g., Green and Ringwood, 1967).

Recent studies of global seafloor basalts demonstrate that lithosphere thickness variation exerts the primary control on the compositions of these basalts, especially those erupted on intraplate ocean islands with varying lithosphere thickness at the time of eruption (Humphreys and Niu, 2009; Niu et al., 2011; Niu, 2016; Niu and Green, 2018). Seafloor basalts erupted on thicker lithosphere have geochemical characteristics of lower extent (*F*) and higher pressure (*P*) of melting, whereas basalts erupted on thinner lithosphere have geochemical signatures of higher *F* and lower *P*. This is because $F \propto P_0 - P_f$, where $P_0$ is the initial depth of melting when the adiabatically upwelling asthenospheric mantle intersects the solidus, and $P_f$ is the depth of melting cessation and melt extraction when the decompression-melting mantle encounters the lithosphere, that is, the depth of the lithosphere-asthenosphere boundary (LAB). This is the concept of the "lid effect" (see Niu et al., 2011), and its mechanism is simply capping decompression melting at the LAB (Niu and Green, 2018). If the lithospheric lid affects oceanic basaltic magmatism, then the lid effect must also affect basaltic magmatism in continental settings, with erupted basalts recording the lid effect as the result of varying lithosphere thickness.

To test the lid effect hypothesis for continental basaltic magmatism, and to evaluate the extent of this effect on the compositional variation of continental basalts, we chose to study Cenozoic basalts in eastern continental China in the Chifeng–Xilin Hot area along a southeast-to-northwest, ~260 km, traverse with a steep topographic gradient (~500 to ~1500 m above sea level) corresponding to a steep lithospheric thickness gradient (~80 to ~120 km). Our finding is fully consistent with the lid effect. We note that source compositional variation and lithospheric contamination can contribute to the compositional variability of continental basalts, but these are secondary and are averaged out, with the mean compositions markedly reflecting the lid effect.

## GEOLOGICAL BACKGROUND

Cenozoic basaltic volcanism is widespread in eastern continental China, from Wudalianchi in the northeast to Hainan Island in the south (Fan and Hooper, 1991). Most of these volcanic rocks are alkali-rich varieties (e.g., Guo et al., 2016; Sun et al., 2017), with tholeiites also present in several locations (Zhi et al., 1990; Zou et al., 2000; Xu et al., 2005). Studies on these continental basalts reveal that they are isotopically depleted relative to the bulk silicate earth, with $\varepsilon_{Nd(t)} > 0$ and $\varepsilon_{Hf(t)} > 0$,

*Current address: Institute of Oceanology, Chinese Academy of Sciences, Nanhai Road 7, Qingdao, Shandong 266071, China; E-mail: guopy@qdio.ac.cn.

CITATION: Guo, P., et al., 2020, Lithosphere thickness controls continental basalt compositions: An illustration using Cenozoic basalts from eastern China: Geology, v. 48, p. 128–133, https://doi.org/10.1130/G46710.1.

but highly enriched in incompatible elements and also enriched in the progressively more-incompatible elements (e.g., Guo et al., 2016; Sun et al., 2017), resembling present-day ocean island basalts (OIBs). The origin of these basalts has been explained as the result of asthenospheric mantle upwelling and decompression melting, which was ultimately caused by the western Pacific wedge suction–induced eastward asthenosphere flow beneath eastern continental China (Niu, 2005, 2014).

The Cenozoic basaltic volcanism in the Chifeng–Xilin Hot area is a type example of Cenozoic volcanism in the region, with its eruption age ranging from ca. 23.8 Ma to ca. 0.19 Ma (Ho et al., 2008; Wang et al., 2015). These basalts spread over a spatial distance of ~260 km across the "Great Gradient Line" (GGL; Niu, 2005), a steep gradient in gravity, elevation, topography, crustal thickness, lithosphere thickness, and heat flow between the high plateaus to the west and the hilly lowland plains in the east (Fig. 1A). Previous studies demonstrated that the distinct contrasts in these geological observations were the result of lithosphere thinning in the region to the east of GGL in the Mesozoic (e.g., Niu, 2005, 2014; Zhu et al., 2011). As shown in Figures 1B and 1C, Chifeng is to the east of the GGL, and Xilin Hot is to the west. Regionally, high-resolution seismic tomography reveals significant changes in the depth of the LAB beneath the Chifeng–Xilin Hot area, ranging from ~80 km beneath Chifeng to ~120 km beneath Xilin Hot (Fig. 1C). This LAB depth also correlates well with the surface elevation (Fig. 1C), reflecting a first-order isostatic equilibrium. The Chifeng–Xilin Hot Cenozoic basalts thus offer a prime opportunity to test the lid effect hypothesis in a continental setting.

## SYSTEMATIC COMPOSITIONAL VARIATIONS OF THE CHIFENG–XILIN HOT BASALTS

We analyzed bulk-rock major element, trace element, and Sr-Nd-Hf isotope on 19 fresh basalt samples from three locations (solid symbols in Fig. 1B). The analytical methods and results are given in the GSA Data Repository[1]. We also used recently published data on 41 basaltic samples from the Chifeng–Xilin Hot area (half-filled symbols in Fig. 1B; Wang et al., 2015; Guo et al., 2016; Pang et al., 2019). In order to remove the effects of fractional crystallization, we corrected major element compositions of all these samples to Mg# = 0.72, the minimum value to be in equilibrium with mantle olivine, following the method of Humphreys and Niu (2009) (see the Data Repository).

[1]GSA Data Repository item 2020xxx, methods, fractionation correction procedure, Figures DR1–DR9, and Tables DR1–DR3, is available online at http://www.geosociety.org/datarepository/2020/, or on request from editing@geosociety.org.

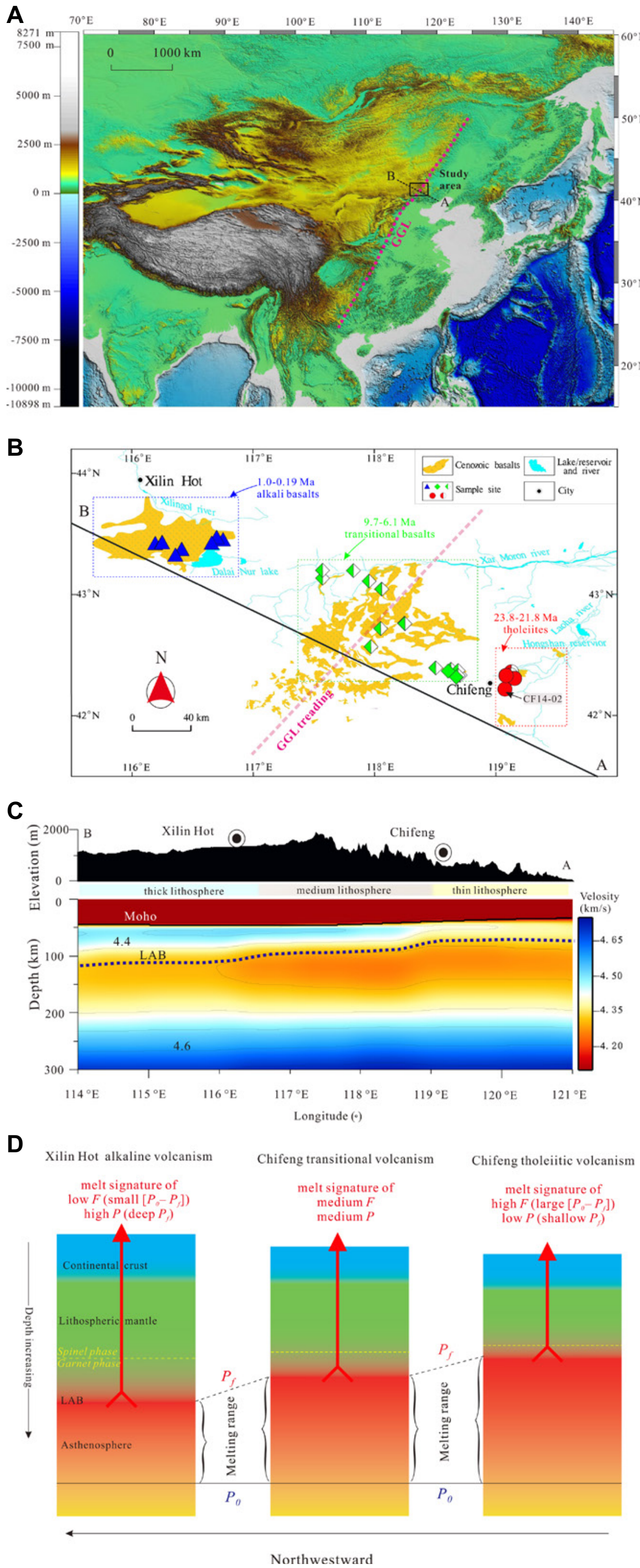


**Figure 1. (A) Topographic map of East Asia (data from Amante and Eakins, 2009). "Great Gradient Line" (GGL) is indicated as purple dashed line, which contrasts high-elevation and thickened lithosphere to the west from low-elevation and thinned lithosphere to the east. Study area is indicated with a rectangle, with the A-B traverse used in subsequent figures. (B) Distribution and sample locations of Chifeng–Xilin Hot Cenozoic basalts. Solid blue triangles, solid green diamonds, and solid red circles represent sample locations in this study. Half-filled diamonds and half-filled circles represent transitional basalt locations from the literature (Wang et al., 2015; Guo et al., 2016; Pang et al., 2019). (C) Top: Topographic profile along the A-B section in A. Bottom: Vertical section of shear-wave velocity tomography along the A-B traverse (based on data of Li et al., 2013). LAB—lithosphere-asthenosphere boundary. (D) Cartoon illustrating lithosphere thickness control on the geochemistry of erupted basaltic magmas. *F*—extent of melting; *P*—melting pressure $P_f$—depth of melting cessation and melt extraction when the decompression-melting mantle encounters the lithosphere, that is, the depth of the lithosphere-asthenosphere boundary; $P_0$—initial depth of melting when the adiabatically upwelling asthenospheric mantle intersects the solidus.**

Spatially, from the southeast to northwest, these basalts change gradually from tholeiite (quartz normative) to transitional basalts (hypersthene normative) to alkali basalts (nepheline normative) (Fig. DR1 in the Data Repository). Figure 2 plots major element compositions corrected to Mg# = 0.72 (notated using the subscript "72" on element symbols) as a function of distance relative to the location of the most southeastern sample (sample CF14-02) calculated using the great-circle distance (e.g., Niu and Batiza, 1993), and shows that $Si_{72}$ decreases while $Mg_{72}$, $Fe_{72}$, $Ti_{72}$, $P_{72}$, and $K_{72}$ increase toward the northwest. Such consistent spatial trends are also obvious for incompatible elements (Fig. DR2), for ratios of highly to moderately

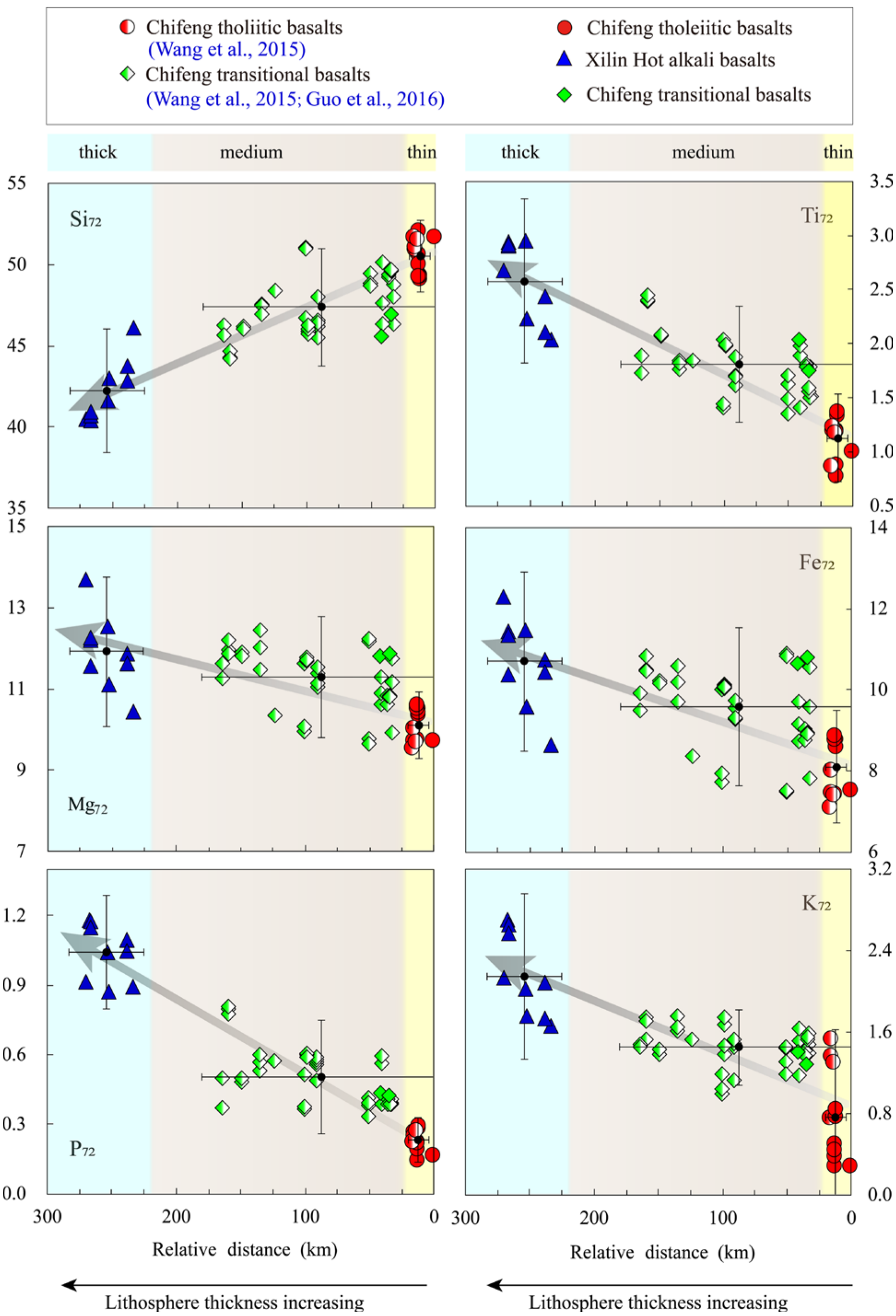


**Figure 2. Systematic variation of major element compositions of Chifeng–Xilin Hot (eastern China) Cenozoic basalts as a function of distance relative to the location of sample CF14-02 parallel to the A-B traverse (Fig. 1B). Relative distance is calculated following the method of Niu and Batiza (1993). Black circles represent average composition, with error bars of 2 standard deviations. Subscript "72" refers to corresponding oxides corrected for the fractionation effect to Mg# = 72 (Humphreys and Niu, 2009) so as to facilitate discussion of mantle sources and processes. Three bands with different colors indicate thick, medium, and thin lithosphere at the time of basalt eruption. Symbols are as in Figure 1B.**

incompatible elements (e.g., $[La/Sm]_N$, where N—primitive mantle normalized; Rb/Hf; Ba/Zr), and for ratios of moderately to slightly incompatible elements (e.g., $[Sm/Yb]_N$, Hf/Lu, Zr/Yb) (Fig. 3). Furthermore, all of these elemental compositions show first-order correlations with topographic elevation (Fig. 4). Despite the high variability in incompatible element composition (Figs. 2–4; Fig. DR2), the Chifeng–Xilin Hot basalts generally display similarly depleted Sr-Nd-Hf isotope compositions relative to the bulk silicate earth, with $^{87}Sr/^{86}Sr$ = 0.70369–0.70443, $^{143}Nd/^{144}Nd$ = 0.512750–0.512931, and $^{176}Hf/^{177}Hf$ = 0.282926–0.283081 (Figs. DR3 and DR4), implying a similar but still heterogeneous mantle source.

## EVALUATION OF CRUSTAL MATERIAL CONTAMINATION

Continental crustal contamination during magma ascent is inevitable, but crustal contamination proxies, such as $SiO_2/MgO$, $K_2O/TiO_2$, $K_2O/P_2O_5$, Ce/Pb, Nb/Th, Ta/U, $^{87}Sr/^{86}Sr$, $^{143}Nd/^{144}Nd$, and $^{176}Hf/^{177}Hf$, show no coherent correlations between each other in our study, suggesting that this effect is negligible (see Fig. DR5). Furthermore, the occurrence of mantle xenoliths carried in Xilin Hot alkaline basalts (Fig. DR6) indicates that the magma ascended rapidly with limited interaction with the crust, which is supported by recent studies (Wang et al., 2015; Guo et al., 2016; Sun et al., 2017; Pang et al., 2019). Therefore, the observed major element and trace element compositional systematics in these basalts (Figs. 2–4) largely reflect those of primary magmas parental to the basalts, as the result of varying source composition or varying extent and pressure of mantle melting.

## EVALUATION OF MANTLE SOURCE COMPOSITIONAL VARIATIONS

Generally, the studied basalts have OIB-like incompatible element compositions with high $[La/Sm]_N$ (1.2–3.5) and $[Sm/Yb]_N$ (2.4–9.2), and are progressively more enriched in the progressively more incompatible elements (Fig. DR7), indicating (1) their derivation from varying low-degree melting of prior metasomatically enriched sources, and (2) the partial melting occurring in the sublithospheric mantle garnet stability field, with garnet as a residual phase. These basalts also show OIB-like depleted Sr-Nd-Hf isotope compositions (Fig. DR3) and elevated $[Nb/Th]_N$ and $[Ta/U]_N$ (Fig. DR8), differing distinctively from those of the >110 Ma alkali basalts in eastern China (Figs. DR3 and DR8), which were derived from melting of the continental lithospheric mantle (e.g., Niu, 2014; Meng et al., 2015). Therefore, these basalts originated from partial melting of metasomatized asthenospheric (versus lithospheric) mantle. Furthermore, the lack of temporal and spatial variation of Sr-Nd-Hf isotopes of these basalts (Fig. DR4) indicates that these basalts have shared a similarly heterogenous asthenospheric mantle source in the Cenozoic.

## LITHOSPHERE THICKNESS EFFECT ON BASALT COMPOSITIONS

In the Chifeng–Xilin Hot area, the lithosphere gradually thickens northwestward (dotted line labeled LAB in Figure 1C). This is mirrored by the increasing surface elevation as the result of isostatic equilibrium; the surface elevation positively correlates with the LAB depth. If the lid effect hypothesis is valid and applies here, we should see systematic variation in the compositions of these basalts as a function of the lithosphere thickness and surface elevation. This is indeed the case (Figs. 2–4).

Figures 2 and 3 show that the Chifeng–Xilin Hot basalts display decreasing $Si_{72}$ but

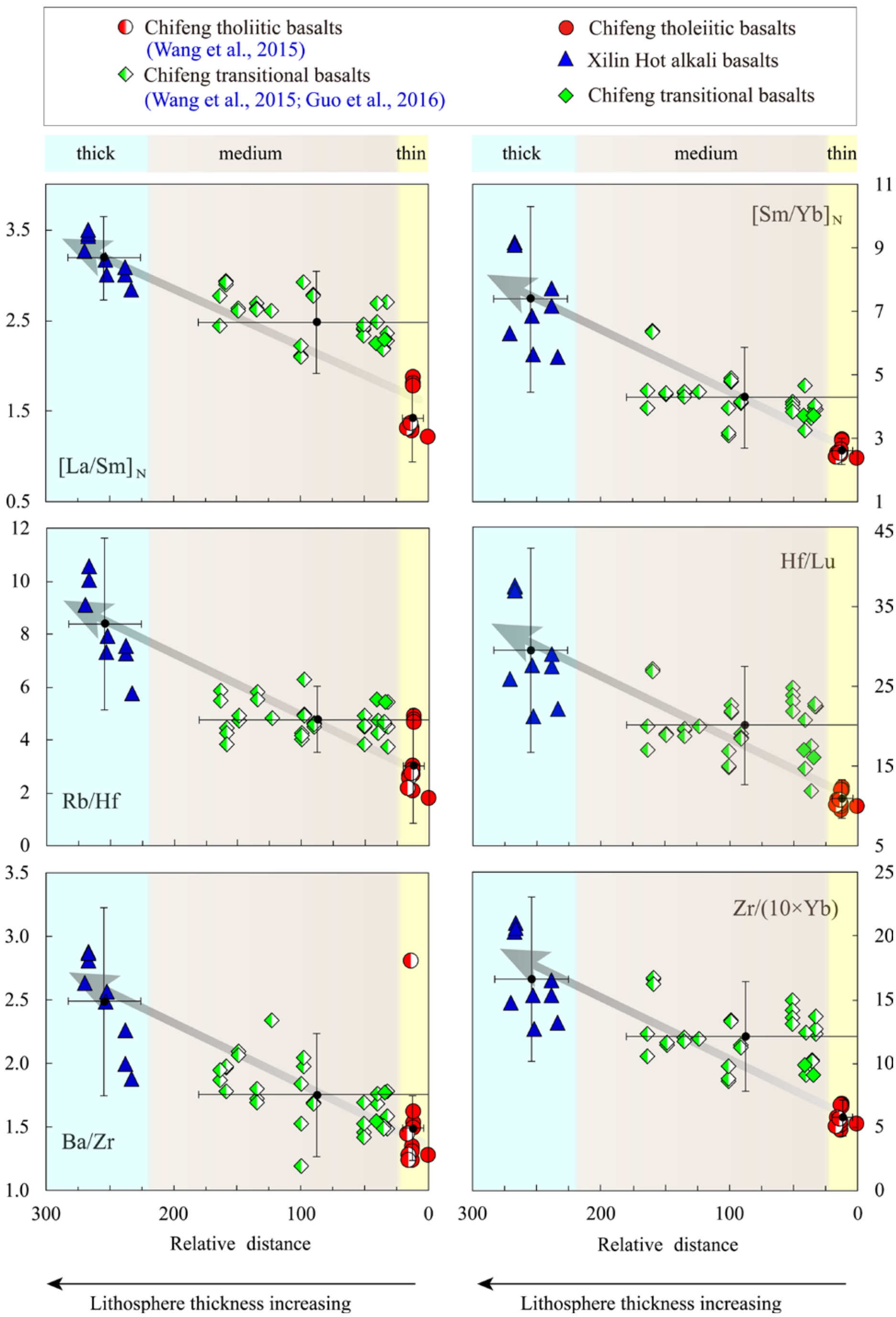


**Figure 3. Systematic variation of ratios of more- to less-incompatible elements of Chifeng–Xilin Hot (eastern China) Cenozoic basalts plotted as function of distance from the location of sample CF14-02 as in Figure 2. Black circles represent average composition, with error bars of 2 standard deviations. Subscript N represents primitive mantle normalized.**

increasing $Mg_{72}$, $Fe_{72}$, and $[Sm/Yb]_N$ with increasing lithosphere thickness toward the northwest, which is consistent with increasing pressure (depth) of melt extraction, $P_f$ (Fig. 1D). $P_f$ corresponds to the thickened lithosphere and is physically the LAB depth (Niu and Green, 2018). Also, toward the northwest, the basalts show an increase in $[La/Sm]_N$, Rb/Hf, Hf/Lu, Ba/Zr, Zr/Yb, $Ti_{72}$, $P_{72}$, $K_{72}$, and other incompatible elements (Figs. 2 and 3; Fig. DR2), which is consistent with the decreasing extent of melting. This is also consistent with the northwestward-thickening lithosphere with a deepening LAB which caps decompression melting and results in melt extraction at greater depths (Fig. 1D). Figure 4 shows the significant correlations of basalt compositions with surface elevation, which further illustrates the lithosphere thickness control (see above). All of these coherent and systematic changes in basalt compositions with lithosphere thickness variation, as well as surface elevation variation, demonstrate the influence of the lid effect on basaltic magmatism in continental settings.

Note that lithosphere thickening due to conductive heat loss to the surface is a natural process (see Niu and Green, 2018). Thus, the lithosphere in the Chifeng–Xilin Hot area would gradually thicken in the Cenozoic, and the erupted magmas would have systematic geochemical variations over the eruption age due to the lid effect, as is shown in Figure DR9. However, a lithosphere with an initial thickness of ~80 km would only thicken by ~13 km due to conductive cooling over the time span of ~20 m.y.; or, to thicken from ~80 km to ~120 km would require ~65 m.y. (see Niu and Green, 2018). Therefore, the ~40 km difference in lithosphere thickness on both sides of the GGL (Fig. 1C) is not caused by conductive cooling. In fact, there is no evidence that the geotherm beneath the region has changed significantly over the past ~22 m.y. (Huang and Xu, 2010). In brief, the systematic compositional variation of the Chifeng–Xilin Hot basalts over time (Fig. DR9) is not caused by lithosphere thickening, but is the result of lithosphere thickness variation along the southeast-to-northwest traverse across the prominent GGL (Figs. 1C and 1D).

## CONCLUSIONS

Studies show that global OIBs vary significantly in their compositions, but the lithosphere thickness (i.e., the depth of the LAB) at the time of OIB eruption exerts the primary control on OIB compositions in terms of the extent and pressure of melting (Humphreys and Niu, 2009; Niu et al., 2011; Niu, 2016; Niu and Green, 2018). This is the "lid effect"; i.e., the lithosphere lid caps the upwelling and decompression melting of mantle, resulting in melts erupted on thin lithosphere having geochemical signatures of a high extent and low pressure of melting, whereas melts erupted on thick lithosphere show the inverse. If the lid effect is globally significant, it should also be true for continental basalts. Our results demonstrate that the lid effect also operates in continental settings. The continental lithosphere thickness (i.e., the LAB depth) exerts the primary control on basaltic compositions in terms of the extent and pressure of melting, and thus is critically important for understating upper mantle dynamics and continental geology. Our results also provide strong evidence for isostatic equilibrium in the crust-mantle system above a mantle depth deeper than the LAB.


## ACKNOWLEDGMENTS

This work was supported by the National Natural Science Foundation of China (grants 41776067, 41630968, and 91014003) and the 111 Project of China (grant B18048). We specially thank Yonghua Li for providing the seismic tomography map of Figure 1C. We are also grateful to Chuanxu Chen, Wanfeng Chen, and Guangxu Zhang for help with geological map and tomography map drawing. We

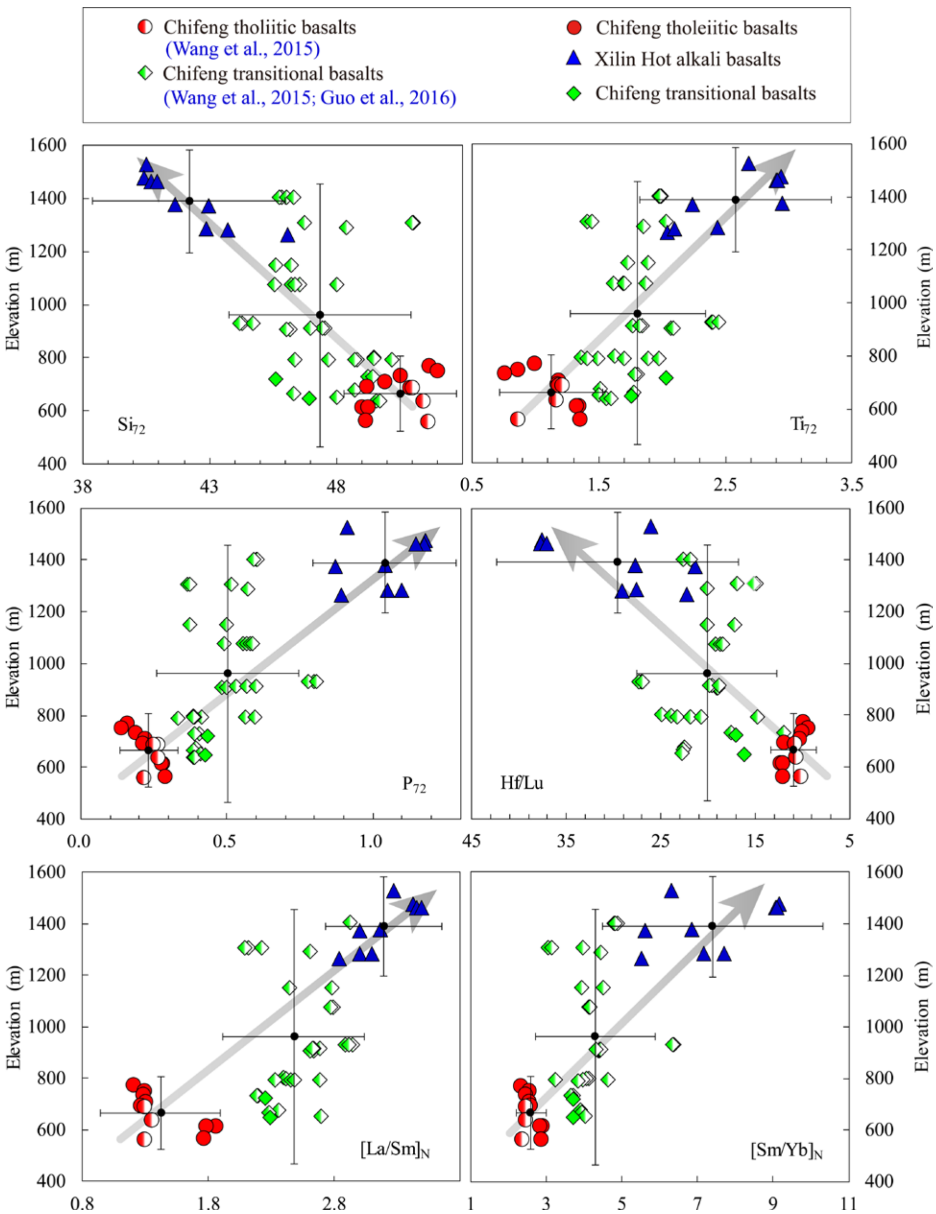


**Figure 4. Systematic variation of major elements and ratios of more- to less-incompatible elements of Chifeng–Xilin Hot (eastern China) Cenozoic basalts with sample (surface) elevation. Black circles represent average composition, with error bars of 2 standard deviations. Subscript N represents primitive mantle normalized; subscript "72" refers to corresponding oxides corrected for fractionation effect to Mg# = 72 (Humphreys and Niu, 2009) so as to facilitate discussion of mantle sources and processes.**

acknowledge editor Chris Clark for handling, and Malcolm Hole and four anonymous reviewers for manuscript reviews.

## REFERENCES CITED


Amante, C., and Eakins, B.W., 2009. ETOPO1 1 arc-minute global relief model: Procedures, data sources and analysis: U.S. National Oceanic and Atmospheric Administration Technical Memorandum NESDIS NGDC-24, 19 p.

Bell, K., and Peterson, T., 1991, Nd and Sr isotope systematics of Shombole volcano, East Africa, and the links between nephelinites, phonolites, and carbonatites: Geology, v. 19, p. 582–585, https://doi.org/10.1130/0091-7613(1991)019<0582:NASISO>2.3.CO;2.

Dupuy, C., and Dostal, J., 1984, Trace element geochemistry of some continental tholeiites: Earth and Planetary Science Letters, v. 67, p. 61–69, https://doi.org/10.1016/0012-821X(84)90038-4.

Ellam, R.M., 1992, Lithospheric thickness as a control on basalt geochemistry: Geology, v. 20, p. 153–156, https://doi.org/10.1130/0091-7613(1992)020<0153:LTAACO>2.3.CO;2.

Fan, Q.C., and Hooper, P.R., 1991, The Cenozoic basaltic rocks of eastern China: Petrology and chemical composition: Journal of Petrology, v. 32, p. 765–810, https://doi.org/10.1093/petrology/32.4.765.

Green, D.H., and Ringwood, A.E., 1967, The genesis of basaltic magmas: Contributions to Mineralogy and Petrology, v. 15, p. 103–190, https://doi.org/10.1007/BF00372052.

Guo, P.Y., Niu, Y.L., Sun, P., Ye, L., Liu, J.J., Zhang, Y., Fang, Y.-x., and Zhao, J.-x., 2016, The origin of Cenozoic basalts from central Inner Mongolia, East China: The consequence of recent mantle metasomatism genetically associated with seismically observed paleo-Pacific slab in the mantle transition zone: Lithos, v. 240, p. 104–118, https://doi.org/10.1016/j.lithos.2015.11.010.

Ho, K.-S., Liu, Y., Chen, J.-C., and Yang, H.-J., 2008, Elemental and Sr-Nd-Pb isotopic compositions of late Cenozoic Abaga basalts, Inner Mongolia: Implications for petrogenesis and mantle process: Geochemical Journal, v. 42, p. 339–357, https://doi.org/10.2343/geochemj.42.339.

Huang, X.L., and Xu, Y.G., 2010, Thermal state and structure of the lithosphere beneath eastern China: A synthesis on basalt-borne xenoliths: Journal of Earth Science, v. 21, p. 711–730, https://doi.org/10.1007/s12583-010-0111-3.

Humphreys, E.R., and Niu, Y.L., 2009, On the composition of ocean island basalts (OIB): The effects of lithospheric thickness variation and mantle metasomatism: Lithos, v. 112, p. 118–136, https://doi.org/10.1016/j.lithos.2009.04.038.

Ingle, S., Scoates, J.S., Weis, D., Brügmann, G., and Kent, R.W., 2004, Origin of Cretaceous continental tholeiites in southwestern Australia and eastern India: Insights from Hf and Os isotopes: Chemical Geology, v. 209, p. 83–106, https://doi.org/10.1016/j.chemgeo.2004.04.023.

Li, Y.H., Wu, Q.J., Pan, J.T., Zhang, F.X., and Yu, D.X., 2013, An upper-mantle S-wave velocity model for East Asia from Rayleigh wave tomography: Earth and Planetary Science Letters, v. 377–378, p. 367–377, https://doi.org/10.1016/j.epsl.2013.06.033.

Lum, C.C.L., Leeman, W.P., Foland, K.A., Kargel, J.A., and Fitton, J.G., 1989, Isotopic variations in continental basaltic lavas as indicators of mantle heterogeneity: Examples from the western U.S. Cordillera: Journal of Geophysical Research, v. 94, p. 7871–7884, https://doi.org/10.1029/JB094iB06p07871.

Meng, F.X., Gao, S., Niu, Y.L., Liu, Y.S., and Wang, X.R., 2015, Mesozoic–Cenozoic mantle evolution beneath the North China Craton: A new perspective from Hf-Nd isotopes of basalts: Gondwana Research, v. 27, p. 1574–1585, https://doi.org/10.1016/j.gr.2014.01.014.

Niu, Y.L., 2005, Generation and evolution of basaltic magmas: Some basic concepts and a new view on the origin of Mesozoic–Cenozoic basaltic volcanism in eastern China: Gaoxiao Dizhi Xuebao, v. 11, p. 9–46.

Niu, Y.L., 2014, Geological understanding of plate tectonics: Basic concepts, illustrations, examples and new perspectives: Global Tectonics and Metallogeny, v. 10, p. 23–46, https://doi.org/10.1127/gtm/2014/0009.

Niu, Y.L., 2016, The meaning of global ocean ridge basalt major element compositions: Journal of Petrology, v. 57, p. 2081–2103, https://doi.org/10.1093/petrology/egw073.

Niu, Y.L., and Batiza, R., 1993, Chemical variation trends at fast and slow spreading mid-ocean ridges: Journal of Geophysical Research, v. 98, p. 7887–7902, https://doi.org/10.1029/93JB00149.

Niu, Y.L., and Green, D.H., 2018, The petrological control on the lithosphere-asthenosphere boundary (LAB) beneath ocean basins: Earth-Science Reviews, v. 185, p. 301–307, https://doi.org/10.1016/j.earscirev.2018.06.011.

Niu, Y.L., Wilson, M., Humphreys, E.R., and O'Hara, M.J., 2011, The origin of intra-plate ocean island basalts (OIB): The lid effect and its geodynamic implications: Journal of Petrology, v. 52, p. 1443–1468, https://doi.org/10.1093/petrology/egr030.

Pang, C.-J., Wang, X.-C., Li, C.-F., Wilde, S.A., and Tian, L.Y., 2019, Pyroxenite-derived Cenozoic basaltic magmatism in central Inner Mongolia, eastern China: Potential contributions from the subduction of the Paleo-Pacific and Paleo-Asian oceanic slabs in the Mantle Transition Zone: Lithos, v. 332, p. 39–54, https://doi.org/10.1016/j.lithos.2019.02.012.

Peterson, T.D., 1989, Peralkaline nephelinites: Contributions to Mineralogy and Petrology, v. 102, p. 336–346, https://doi.org/10.1007/BF00373727.

Sun, P., Niu, Y.L., Guo, P.Y., Ye, L., Liu, J.J., and Feng, Y.X., 2017, Elemental and Sr-Nd-Pb isotope geochemistry of the Cenozoic basalts in Southeast China: Insights into their mantle sources and melting processes: Lithos, v. 272, p. 16–30, https://doi.org/10.1016/j.lithos.2016.12.005.

Wang, X.-C., Wilde, S.A., Li, Q.-L., and Yang, Y.-N., 2015, Continental flood basalts derived from the hydrous mantle transition zone: Nature Communications, v. 6, 7700, https://doi.org/10.1038/ncomms8700.

Xu, Y.-G., Ma, J.-L., Frey, F.A., Feigenson, M.D., and Liu, J.-F., 2005, Role of lithosphere-asthenosphere interaction in the genesis of Quaternary alkali and tholeiitic basalts from Datong, western North China Craton: Chemical Geology, v. 224, p. 247–271, https://doi.org/10.1016/j.chemgeo.2005.08.004.

Zhi, X.C., Song, Y., Frey, F.A., Feng, J.L., and Zhai, M.Z., 1990, Geochemistry of Hannuoba basalts, eastern China: Constraints on the origin of continental alkalic and tholeiitic basalt: Chemical Geology, v. 88, p. 1–33, https://doi.org/10.1016/0009-2541(90)90101-C.

Zhu, R.X., Chen, L., Wu, F.Y., and Liu, J.L., 2011, Timing, scale and mechanism of the destruction of the North China Craton: Science China: Earth Sciences, v. 54, p. 789–797, https://doi.org/10.1007/s11430-011-4203-4.

Zou, H.B., Zindler, A., Xu, X.S., and Qu, Q., 2000, Major, trace element, and Nd, Sr and Pb isotopic studies of Cenozoic basalts in SE China: Mantle sources, regional variations, and tectonic significance: Chemical Geology, v. 171, p. 33–47, https://doi.org/10.1016/S0009-2541(00)00243-6.

Printed in USA